Astron. Astrophys. 321, 850–858 (1997)

ASTRONOMY AND ASTROPHYSICS

Coronal X-ray emission of HD 35850: the ASCA view

G. Tagliaferri[1], **S. Covino**[1], **T.A. Fleming**[2], **M. Gagné**[3], **R. Pallavicini**[4], **F. Haardt**[5], **and Y. Uchida**[6]

[1] Osservatorio Astronomico di Brera, via E. Bianchi 46, I-22055 Merate (LC), Italy
[2] Steward Observatory, University of Arizona, Tucson, Arizona, USA
[3] JILA, University of Colorado, Boulder, CO 80309-0440, USA
[4] Osservatorio Astronomico G.S. Vaiana, Palermo, Italy
[5] Institute of Theoretical Physics, Chalmers University Technology, S-41296 Göteborg, Sweden
[6] Science University of Tokyo, Tokyo, Japan

Received 6 September 1996 / Accepted 5 November 1996

Abstract. We present the analysis of the X–ray data of the young active star HD 35850 obtained with ASCA and ROSAT. Our main goal was to see if there is a difference in the elemental abundances of active stars between young and more evolved objects. A two temperature plasma with subsolar abundances, of the order of $Z = 0.15 - 0.3$, is required to fit the SIS spectra. Similar results are obtained from a ROSAT PSPC observation. Metal abundances of 0.2 – 0.4 the solar value are required to fit both the ASCA and ROSAT data together. From a simultaneous SIS0+SIS1 spectral fit, with 2T plasma models and abundances free to vary in non-solar proportions, we find that, besides N, O and Ne for which we find very low values, all other elements have values relative to solar abundances around 0.2–0.3. These subsolar abundances are in line with those typically observed in more evolved, active stars like RS CVn and Algol–type binaries.

The two temperature values required to fit the ASCA SIS spectra are about 0.5 and 1.0 keV. These temperatures, especially the higher one, are lower with respect to the values found for the RS CVn and Algol binaries or for the young star AB Dor, but higher than other single G/K stars. All our data show that this single, late F–type star is actually a very active source, indirectly confirming that this fast rotating star is probably a young object. In the simultaneous fit of the ASCA+ROSAT data, a third temperature is required. However this is not just an addition of a softer component, but is more a redistribution of the dominant temperatures. Indeed, the range spanned by the three temperatures, from 5 to 15 million degrees, is not very large.

Key words: X-ray: stars – stars: abundances – stars: activity – stars: coronae – stars: individual: HD 35850

1. Introduction

The decline of coronal emission with age is commonly interpreted to be a consequence of reduced magnetic activity during the course of stellar evolution. Mass loss through magnetized stellar winds progressively decreases the star rotation rate, and this in turn makes the generation of surface magnetic fields by the dynamo process less efficient. By studying X–rays from stars of different age one has a powerful tool to investigate coronal emission under different conditions of magnetic activity.

The spectral capabilities of ASCA now have the potential to study in some detail the X–ray spectra of a sizable number of stars at different levels of activity and/or age. However, late–type stars in galactic clusters and star–forming regions are typically too far away to be studied at sufficiently high signal–to–noise ratio (S/N) with ASCA. Fortunately, a number of nearby isolated young stars which can be used as good proxies for cluster members, have been discovered recently. These objects have been identified on the basis of various criteria, including rapid rotation, enhanced X–ray emission (e.g. Vilhu et al. 1987), large Li abundances (Pallavicini et al. 1992a, 1992b, Randich et al. 1993), space motions indicative of membership in associations (Innis et al. 1968, Anders et al. 1991), or a combination of the above criteria. The most effective way to discover isolated young stars (i.e. NOT in star forming regions) is probably through X–ray and EUV surveys as demonstrated by optical follow–up observations of serendipitous X–ray sources detected with *Einstein*, EXOSAT, ROSAT and EUVE (Fleming et al. 1988, 1989; Tagliaferri et al. 1992a, 1992b, 1994; Favata et al. 1993; Jeffries 1995).

We have carried out extensive photometric and spectroscopic observations of the optical counterparts of stellar X–ray sources discovered serendipitously by EXOSAT (Tagliaferri et al. 1992a, 1992b, 1994; Cutispoto et al. 1995) and found that at least one third of the EXOSAT serendipitous sources are, in fact, young stars with ages comparable to or younger than the Pleiades ($\sim 7 \times 10^7$ yrs). Here we present an ASCA observation of one of these stars, HD 35850.

HD 35850 is a single star of spectral type F8/9 V with a spectroscopic distance $\sim$ 24 pc (Cutispoto et al. 1995). The source was detected serendipitously by EXOSAT with an intrinsic X–ray luminosity of $\sim 1.6 \times 10^{30}$ erg s^{-1}. This value

Send offprint requests to: G. Tagliaferri

is quite remarkable for a single, late F–type star and one might suspect the presence of a less massive companion in order to explain its high X–ray luminosity. However, our optical data seem to confirm that HD 35850 is a true single star. We observed this source for six consecutive nights taking high resolution spectra (R=50000, S/N$>$ 100) every night in the H_α region. We found a constant radial velocity (V_r = 24 $\pm$ 2.4 Km s^{-1}) over the six nights. This leads us to exclude that the star is a short period spectroscopic binary (Pastori et al. 1996). The source has been detected again by both the ROSAT–WFC and EUVE all–sky surveys, and as a serendipitous source in a ROSAT–PSPC pointing (Panarella et al. 1996). The large Li abundance [$\log n(Li)$ = 3.2, comparable to the protostellar Li abundance of Pop I stars], solar metallicity, and large rotation rate ($v \sin i$ = 50 km s^{-1}) are all consistent with HD 35850 being a young object, at least as young as the Pleiades (Tagliaferri et al. 1994).

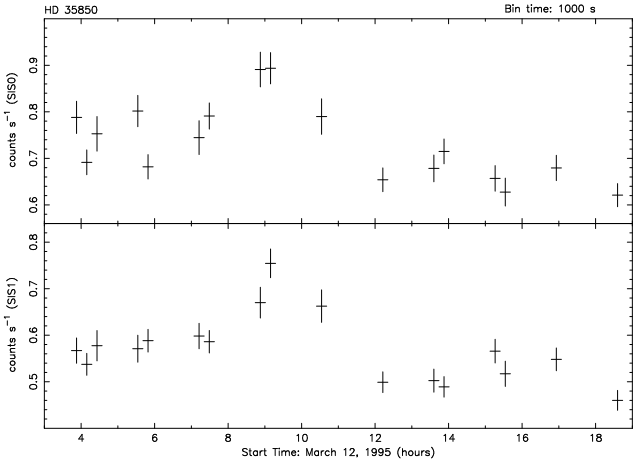

Fig. 1. SIS light curves of HD 35850; a variability of the order of $\sim$ 20% is detected.

2. Observations and results

The Advanced Satellite for Cosmology and Astrophysics (ASCA) is an X–ray observatory carrying four detectors onboard, namely two Solid State Imaging Spectrometers (SIS) and two Gas Imaging Spectrometers (GIS). Each detector is at the focus of an imaging thin foil grazing incidence telescope (Tanaka et al. 1994). Each SIS has four CCD chips, but for our observation they were operated in 1–CCD mode, that implies a field of view (FOV) of $11' \times 11'$. The FWHM energy resolution of each SIS is $\sim$ 60–120 eV from 1–6 keV, compared to 200–600 eV for the GIS. Each GIS has a $40'$ diameter circular field of view. SIS0 and GIS2 are the two best calibrated detectors. The observation of HD 35850 started on 1995 March 12 at 02:20 and ended at 19:20.

2.1. Light curves

Using an extraction radius of 4 arcmin, the background subtracted source count rates are 0.701 $\pm$ 0.007 for SIS0 and 0.200 $\pm$ 0.004 $cts\ s^{-1}$ for GIS2. The total good exposure time was 18 ksec. The light curves from the 4 different detectors have been analysed. In Fig. 1 we show the rebinned SIS light curves with a 1000 sec/bin stepsize. Bins containing less than 500 sec of exposure time have been excluded. In all four detectors, the count rate is not consistent with a constant source, with flux variations of $\simeq$ 20% on timescales of a few hours at the 3–σ level in the two SIS datasets (Fig. 1). In order to test for a possible energy dependence of the count rate variation, we have produced separate light curves of the SIS datasets for the low–energy channels (0.5–0.9 keV) and for the high–energy channels (1.1–4 keV). No significant change in the hardness ratio compatible with the statistics of our data has been found. The statistical significance of any flux change in the GIS datasets is lower, closer to 1–σ.

2.2. Spectral analysis

Since the hardness ratio is essentially constant for the duration of the observation, we have performed the spectral analysis using the whole data set without any time filtering. The extracted spectra have been rebinned to give at least 25 counts per bin. A background spectrum was accumulated from the outer regions of the field of view (FOV) for the GIS detectors. For the SIS detectors, we used the standard background data provided by the ASCA observatory team since our source almost completely fills the 1CCD mode FOV. Of course, this procedure can only be followed if the background is constant, which indeed was the case.

While analyzing our ASCA data, we encountered several problems. In particular, although we tried various procedures, we never obtained statistically fully satisfactory spectral fits for the SIS detectors. This could be partly attributed to uncertainties in some of the models used (see below) and/or in detector calibration. We now give a summary of the tests we performed during the data analysis. Then we will concentrate on the results obtained. In order to estimate the uncertainties on the PSF calibration, we extracted SIS spectra using two different circle sizes, i.e. with a smaller circle implying a larger PSF correction. We used a radius of 38 original pixels and another of 150 original pixels (130 for SIS1). The larger circle is the one suggested by the ASCA observatory team (for SIS1 we had to use a slightly smaller radius as the source is not centered in the 1CCD detector FOV). All fits with different models, detector combinations, and energy ranges (by ignoring channels) were performed on both spectra extracted using both circle sizes. As a result, we found that the best–fit values for the temperatures and abundances are quite similar in the two cases, but they are better constrained for the larger extraction radius, although in this case the fits are statistically less satisfactory (i.e. the reduced χ^2 is always larger). The formally better fits obtained with the smaller extraction radius are probably due to the larger statistical errors associated with the energy bins, given that us-

Table 1. Fit parameters for SIS0 and SIS1. They are computed for RS and MK models, 2 or 3 components and with abundances fixed at the solar value or free to vary in solar proportion. Errors are at 90% confidence for 2 or 3 parameters of interest.

SIS0	T_1 KeV	E.M.$_1$ (10^{52} cm^{-3})	T_2 KeV	E.M.$_2$ (10^{52} cm^{-3})	T_3 KeV	E.M.$_3$ (10^{52} cm^{-3})	Z	χ^2_ν	*d.o.f.*
RS	$0.76\pm^{0.02}_{0.02}$	2.62	$1.75\pm^{0.33}_{0.23}$	1.71	–	–	1	2.89	101
”	$0.35\pm^{0.03}_{0.04}$	0.93	$0.80\pm^{0.03}_{0.03}$	2.11	$1.91\pm^{0.58}_{0.32}$	1.72	1	2.28	99
”	$0.44\pm^{0.19}_{0.10}$	2.87	$0.79\pm^{0.04}_{0.03}$	12.6	–	–	$0.15\pm^{0.03}_{0.03}$	1.37	100
MK	$0.63\pm^{0.02}_{0.01}$	2.75	$1.94\pm^{0.31}_{0.23}$	1.94	–	–	1	2.60	100
”	$0.48\pm^{0.07}_{0.07}$	1.48	$0.77\pm^{0.08}_{0.06}$	1.62	$2.25\pm^{0.16}_{0.33}$	1.75	1	2.14	99
”	$0.63\pm^{0.02}_{0.08}$	11.7	$1.16\pm^{1.04}_{0.33}$	2.99	–	–	$0.18\pm^{0.07}_{0.04}$	1.53	100
SIS1	T_1 KeV	E.M.$_1$ (10^{52} cm^{-3})	T_2 KeV	E.M.$_2$ (10^{52} cm^{-3})	T_3 KeV	E.M.$_3$ (10^{52} cm^{-3})	Z	χ^2_ν	*d.o.f.*
RS	$0.51\pm^{0.16}_{0.04}$	1.04	$1.03\pm^{0.02}_{0.03}$	3.16	–	–	1	2.57	92
”	$0.43\pm^{0.08}_{0.08}$	0.72	$0.86\pm^{1.40}_{0.00}$	2.31	$1.75\pm^{0.39}_{0.40}$	1.44	1	2.19	90
”	$0.59\pm^{0.09}_{0.17}$	3.55	$0.91\pm^{0.00}_{0.05}$	8.22	–	–	$0.23\pm^{0.09}_{0.06}$	1.63	91
MK	$0.64\pm^{0.02}_{0.02}$	2.36	$1.43\pm^{0.13}_{0.10}$	2.09	–	–	1	1.70	92
”	$0.59\pm^{0.05}_{0.09}$	1.93	$0.97\pm^{1.33}_{0.24}$	1.09	$1.88\pm^{2.98}_{0.40}$	1.56	1	1.57	90
”	$0.63\pm^{0.02}_{0.04}$	6.04	$1.16\pm^{0.14}_{0.12}$	3.91	–	–	$0.32\pm^{0.14}_{0.08}$	1.20	91

Table 2. Fit parameters for GIS2 and GIS3. They are computed for RS and MK models, 1 or 2 components and with abundances fixed at the solar value or free to vary in solar proportion. Errors with 90% confidence for 2 parameters of interest.

GIS2	T_1 (KeV)	E.M.$_1$ (10^{52} cm^{-3})	T_2 (KeV)	E.M.$_2$ (10^{52} cm^{-3})	Z	χ^2_ν	*d.o.f.*
RS	$0.65\pm^{0.12}_{0.16}$	1.62	$1.30\pm^{0.34}_{0.22}$	1.94	1	0.79	111
”	$0.73(\pm^{0.07}_{0.07})$	13.8	–	–	$0.12(\pm^{0.09}_{0.05})$	0.68	112
MK	$0.61\pm^{0.08}_{0.09}$	2.20	$1.53\pm^{0.32}_{0.20}$	1.73	1	0.81	111
”	$0.68\pm^{0.07}_{0.07}$	16.4	–	–	$0.11\pm^{0.06}_{0.04}$	1.05	112
GIS3	T_1	E.M.$_1$	T_2	E.M.$_2$	Z	χ^2_ν	
RS	$0.78\pm^{0.04}_{0.45}$	2.39	$1.69\pm^{1.88}_{0.57}$	1.40	1	0.78	125
”	$0.80\pm^{0.04}_{0.05}$	10.7	–	–	$0.21\pm^{0.12}_{0.08}$	0.78	126
MK	$0.62\pm^{0.09}_{0.11}$	2.38	$1.56\pm^{0.40}_{0.23}$	1.95	1	0.74	125
”	$0.74\pm^{0.07}_{0.06}$	1.36	–	–	$0.16\pm^{0.08}_{0.05}$	0.83	126

ing a smaller circle implies fewer counts per bin. The higher S/N spectra amplify the uncertainties in the SIS calibration and in the spectral models. Also, we should point out that two different normalizations for every component are necessary to fit the two SIS spectra extracted in the smaller circle (one for each detector), while they are not required for the larger circle SIS spectra. This immediately shows that the PSF uncertainties are reduced by using the larger circle. In the following discussion, we will concentrate only on the larger circle SIS spectra.

The low–energy channels contribute most to the χ^2. It is already known that there are particular problems with the calibration of the SIS detectors below 0.55 keV. To test the influence of the low–energy channels on the spectral fit results, we systematically fitted the SIS0 spectrum by gradually increasing the low–energy cut-off (SIS0 is the better calibrated between the two SISs). The lowest energy values considered in the various cases are 0.3, 0.55, 0.7 and 0.8 keV. We found that the reduced χ^2 significantly improves each time we removed the lowest energy bins. The elemental abundance value in solar proportion (Anders & Grevesse 1989) goes from essentially solar to very low value as the low–energy limit goes from 0.3 to 0.55 keV. Although any further increase of the low–energy limit does not significantly change the abundance value, it does cause a change in the temperature values. In fact, the second temperature component is not constrained any longer and, indeed, a single intermediate temperature is sufficient to fit the data. Based on these results, we decided to use 0.55 keV as the lower energy limit.

A similar problem arose for the channels above 4 keV. In all four detectors, the count rates in the high–energy channels are systematically in excess of the various best–fitted models. Being common to all four detectors, such an excess could be intrinsic to the source spectrum, but it could also be due to uncertainties in the data and/or in the calibration. As a matter of fact, there are few bins above 4 keV and they have large errors due to the low count rate at high–energy (we rebinned the spectrum to have at least 25 counts per bin). We then decided to ignore all the energy channels above 4 keV, since they have a limited influence on the fits.

Finally, we computed the errors in our model fitting using two different statistical methods. In our spectra, the counts in each bin go from 25 to a few hundred and standard Poissonian statistics should be fairly adequate. However, these counts also include the background contribution. Thus, in the background subtracted spectra, there could be some bins with too low a count rate to properly apply Poissonian statistics. Special statistics with $\sigma = (1 + \sqrt{N + 0.75})$ is found to be better suited when the number of counts N is small (Gehrels 1986). When N is large, the two are essentially the same. We performed extensive tests with the XSPEC package (version 9.01) using statistical errors computed with the two procedures and we found that the best–fit parameters in non–critical situations (e.g. when the best–fit parameters are well defined) are almost identical, although in some special cases they are better constrained using the second statistical method. In particular, this non–standard way of weighting, as expected, is less sensitive to the channels above $\sim$ 4 keV, which have the lowest number of counts. In addition, χ^2 is lower, but again this is not surprising since the error bars are larger. In the following, we use the second statistical method. However, it is worth pointing out that no difference in the results obtained with the two statistical methods was found after we restricted the SIS intervals between 0.55–4 keV.

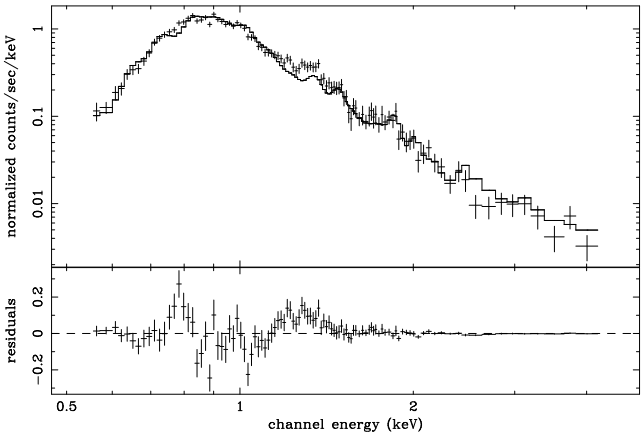

Fig. 2. Fit of the best calibrated SIS detector, SIS0, with a 3–temperature MK model and abundances fixed to the solar value. Note the structures in the residuals; assuming solar abundance clearly does not fit the data even with a 3T model.

For the spectral analysis, we used the optically thin plasma models by Raymond & Smith (RS, 1977) and Mewe et al. (MK, 1996a), also known as "mekal", as implemented inside XSPEC. Emission measures were defined as E.M. = $\int n^2\, dV$ and E.M. = $\int n_e n_H\, dV$ for RS and MK models, respectively. In all models, the column density N_H was fixed at 1×10^{18} cm^{-2} as determined from the EUVE data (Gagné et al. 1996). A two-temperature model with solar abundances gives unacceptable fits to the SIS spectra. A clear improvement is obtained either by adding a third temperature component or by allowing the abundances to vary (in solar proportion). The latter model gives much better fits with subsolar abundances ($Z \simeq 0.15 - 0.3$; see Table 1), while the former is still unacceptable. In Fig. 2, we plot the SIS0 spectrum together with the best–fitted 3T MK model with abundances fixed at the solar value. Note the structures in the residuals, which immediately show that a solar value for the abundances does not allow a good fit to the data. However, in no case are our fits to the data fully satisfactory (see Table 1). Given the statistics of our data, we did not try a 3T model with variable abundances.

The spectra obtained with the two GIS cameras have lower spectral resolution and are also noisier. A good fit to the GIS data is obtained both with $2T$ models with solar abundances or with $1T$ models with lower–than–solar abundances. In the latter case, the abundance values are very similar to those obtained with the SISs (Table 2).

We then performed simultaneous fits by combining the best calibrated detectors, namely SIS0+GIS2, or the spectra with the highest resolution, namely SIS0+SIS1. In the first case, we considered 2T and 3T models with metal abundances either fixed to solar or free to vary in solar proportions. The inclusion of more

Table 3. Fit parameters for SIS0+SIS1. They are computed for RS and MK models with 2 components and variable abundances. Abundances errors are based on χ^2_{min} + 2.71.

	RS	MK
T_1 (KeV)	$0.50\pm^{0.03}_{0.02}$	$0.57\pm^{0.02}_{0.04}$
E.M.$_1$ (10^{52} cm^{-3})	6.56	7.19
T_2 (KeV)	$0.95\pm^{0.02}_{0.11}$	$1.00\pm^{0.05}_{0.08}$
E.M.$_2$ (10^{52} cm^{-3})	7.26	5.07
N	$0 (< 0.74)$	$0 (< 2.33)$
O	$0.04\pm^{0.00}_{0.04}$	$0.06\pm^{0.05}_{0.05}$
Ne	$0.06\pm^{0.00}_{0.06}$	$0.01\pm^{0.06}_{0.01}$
Mg	$0.19\pm^{0.07}_{0.07}$	$0.35\pm^{0.06}_{0.08}$
Si	$0.18\pm^{0.03}_{0.06}$	$0.23\pm^{0.07}_{0.05}$
S	$0.17\pm^{0.00}_{0.12}$	$0.24\pm^{0.14}_{0.14}$
Fe	$0.17\pm^{0.04}_{0.04}$	$0.25\pm^{0.03}_{0.04}$
Ni	$1.18\pm^{0.37}_{0.38}$	$0.39\pm^{0.32}_{0.26}$
χ^2_ν	1.42	1.33
d.o.f.	189	189

spectral bins seems to formally improve the average quality of the fits as measured by the χ^2 values. This analysis confirms the results obtained with SIS0 alone. The fit parameters are essentially the same with somewhat smaller 90%–confidence limits. In the second case, SIS0+SIS1, we considered a $2T$ model with variable abundances. As can be seen from Table 3, there is quite good agreement between the RS and MK models. They both have a very low value of N, O and Ne. All other elements are around 0.2–0.3, except Ni, which has a higher value in the RS model while it is similar to the other elements in the MK model.

2.3. ROSAT data

We also considered ROSAT PSPC data of HD 35850 taken from the public archive. HD 35850 was serendipitously detected during a PSPC observation of more than 5000 s carried out in March 1992. It had a PSPC count rate of 2.8 $cts\ s^{-1}$ for a total of more than 14000 counts in the spectrum. We fitted the PSPC spectrum with a 2T (RS and MK) model plus the N_H fixed at the EUVE value. We note that ROSAT, in contrast with ASCA, is quite sensitive to the N_H, so the assumed N_H value has an important impact on the other parameters. We could have also chosen to fit this parameter but, if we wish to allow the abundances to vary, then there would be too many free parameters given the (low) statistics of our spectrum and the poor ROSAT spectral resolution. Since EUVE is very good in determining the N_H, we preferred to use the N_H value as determined with EUVE. As can be seen from Table 4, if we assume solar abundances, statistically, the best–fit is not fully satisfactory with a reduced χ^2 of 1.6 and 1.4 with RS and MK respectively (48 degree of freedom – dof). If we allow the abundance to vary in solar proportion, the best–fit value for the abundance is 0.3–0.4 for the two models, respectively. An F–test shows that the improvement of the χ^2 is significant at more than 99%. However, the two temperatures, which increased, are not well constrained any more by the ROSAT data alone. It is in any case encouraging that both the temperatures and the abundance values are in good agreement with the ASCA ones. However, with the abundances fixed to solar value, the cooler ROSAT temperature is a factor of three lower than the ASCA one. Similar temperature values, with assumed solar abundances, are commonly found for active stars with ROSAT (e.g. Dempsey et al. 1993).

The 0.5–2.0 keV source flux in the two observations (ASCA and ROSAT) is at similar levels within the errors, i.e. $\sim$ 1.3 and 1.4×10^{-11} erg cm^{-2} s^{-1} respectively, corresponding to an X–ray luminosity of $\sim$ 1.5×10^{30} erg s^{-1} in the 0.5–2.0 keV energy band. Thus, we decided to simultaneously fit the PSPC+SIS0+GIS2 data of HD 35850 (Fig. 3). To fit the data we had to use a 3T model, while the metal abundances were either kept fixed at solar values or free to vary in solar proportion. Because the ROSAT and ASCA observations are not simultaneous, we also allowed different ROSAT and ASCA normalizations. The results are reported in Table 5. It is clear that a plasma with solar abundances can not fit the data. Adding together the RS and MK intervals, at a 90% confidence level, the metal abundance value is determined to be between 0.2–0.4. The two cooler temperatures are well–constrained, while the warmest component at 1.6–1.9 keV is less precisely defined (Table 5). If we allow for different normalizations between ROSAT and ASCA, then an F–test shows that the best–fit improvement is statistically significant at more than a 99% level in all cases (RS and MK, solar and non–solar abundances). However, all other parameters (temperatures and abundances) are essentially the same (see Table 5). Since the fluxes estimated during the two observations are similar and since the ratios of the three normalizations between the two missions are different with no systematic trend, the need of different normalizations between ROSAT and ASCA is probably due to detector calibration uncertainties rather than to source variability.

3. Discussion

Our main goal was to see if there is a difference in the elemental abundances between very active young stars, as HD 35850 should be, and more evolved active stars such as the RS CVn–type binaries.

In the fits of the SIS spectra, all models with solar abundance (2T and 3T RS or MK) that we considered do not give acceptable fits. Instead, a 2T model with abundances free to vary in solar proportion gives much better fits, although statistically not fully satisfactory, with most of the χ^2 contribution arising from the structures between 0.7 and 1.1 keV. This is probably due to either an inaccurate calibration of the SIS detectors or to uncertainties and/or inaccuracies in the current plasma models, which are below the noise in the low–energy resolution GIS spectra, but could well affect the higher resolution SIS data. In fact, there is growing evidence that plasma codes fail to some degree to model the cool star spectra obtained with both the EUVE and ASCA satellites. Theoretical and/or numerical improvements are thus required in the commonly used thin plasma models

Table 4. Fit parameters for the ROSAT PSPC data. They are computed for RS and MK models with abundances fixed at the solar value or free to vary in solar proportion. Errors with 90% confidence are given for 2 or 3 parameters of interest.

ROSAT	T_1 (KeV)	E.M.$_1$ (10^{52} cm^{-3})	T_2 (KeV)	E.M.$_2$ (10^{52} cm^{-3})	Z	χ^2_ν	*d.o.f.*
RS	$0.20\pm^{0.04}_{0.03}$	1.31	$0.80\pm^{0.06}_{0.05}$	3.16	1	1.64	48
”	$0.63\pm^{0.07}_{0.37}$	6.98	$1.28\pm^{\infty}_{0.50}$	3.08	$0.29\pm^{0.25}_{0.06}$	1.39	47
MK	$0.20\pm^{0.04}_{0.04}$	1.15	$0.73\pm^{0.10}_{0.05}$	3.41	1	1.41	48
”	$0.47\pm^{\infty}_{0.26}$	4.79	$0.93\pm^{\infty}_{0.00}$	4.11	$0.42\pm^{0.23}_{0.10}$	1.23	47

Table 5. Fit parameters for SIS0+GIS2+PSPC. They are computed for RS and MK models, with 3 components and abundances fixed at the solar value or free to vary in solar proportion. We considered the case with free normalizations between the ROSAT and ASCA data for each component and the case with a single normalization for both datasets for each component. Errors with 90% confidence are given for 3 or 4 parameters of interest.

RS	Free	normaliz.	ASCA norm. =	ROSAT norm.
	Solar ab.	Non–sol. ab.	Solar ab.	Non–sol. ab.
T_1	$0.20\pm^{0.06}_{0.01}$	$0.35\pm^{0.10}_{0.06}$	$0.19\pm^{0.01}_{0.03}$	$0.36\pm^{0.08}_{0.04}$
E.M.$_1$ (SIS0+GIS2)	0.75×10^{52}	2.21×10^{52}	1.17×10^{52}	2.32×10^{52}
E.M.$_1$ (PSPC)	1.25×10^{52}	1.94×10^{52}	–	–
T_2	$0.74\pm^{0.03}_{0.02}$	$0.68\pm^{0.07}_{0.04}$	$0.74\pm^{0.03}_{0.04}$	$0.79\pm^{0.04}_{0.06}$
E.M.$_2$ (SIS0+GIS2)	2.18×10^{52}	4.45×10^{52}	2.23×10^{52}	5.87×10^{52}
E.M.$_2$ (PSPC)	2.34×10^{52}	8.92×10^{52}	–	–
T_3	$1.65\pm^{0.33}_{0.18}$	$0.99\pm^{1.13}_{0.05}$	$1.65\pm^{0.33}_{0.26}$	$1.61\pm^{1.35}_{0.44}$
E.M.$_3$ (SIS0+GIS2)	1.56×10^{52}	4.69×10^{52}	1.56×10^{52}	1.43×10^{52}
E.M.$_3$ (PSPC)	1.60×10^{52}	1.20×10^{52}	–	–
Z	1	$0.25\pm^{0.05}_{0.03}$	1	$0.34\pm^{0.04}_{0.05}$
χ^2_ν	2.25	1.73	2.45	1.84
d.o.f.	258	257	261	260
MK	Free	normaliz.	ASCA norm. =	ROSAT norm.
	Solar ab.	Non–sol. ab.	Solar ab.	Non–sol. ab.
T_1	$0.17\pm^{0.02}_{0.04}$	$0.53\pm^{0.07}_{0.09}$	$0.15\pm^{0.02}_{0.04}$	$0.52\pm^{0.07}_{0.07}$
E.M.$_1$ (SIS0+GIS2)	0.33×10^{52}	4.37×10^{52}	0.68×10^{52}	4.64×10^{52}
E.M.$_1$ (PSPC)	0.72×10^{52}	4.76×10^{52}	–	–
T_2	$0.63\pm^{0.02}_{0.02}$	$0.78\pm^{0.19}_{0.10}$	$0.62\pm^{0.02}_{0.02}$	$0.78\pm^{0.15}_{0.09}$
E.M.$_2$ (SIS0+GIS2)	2.63×10^{52}	3.30×10^{52}	2.75×10^{52}	3.64×10^{52}
E.M.$_2$ (PSPC)	2.95×10^{52}	4.26×10^{52}	–	–
T_3	$1.78\pm^{0.23}_{0.16}$	$1.83\pm^{0.85}_{0.36}$	$1.80\pm^{0.23}_{0.16}$	$1.90\pm^{1.00}_{0.38}$
E.M.$_3$ (SIS0+GIS2)	1.71×10^{52}	1.71×10^{52}	1.69×10^{52}	1.57×10^{52}
E.M.$_3$ (PSPC)	1.60×10^{-3}	0.57×10^{-3}	–	–
Z	1	$0.35\pm^{0.06}_{0.04}$	1	$0.34\pm^{0.04}_{0.03}$
χ^2_ν	2.03	1.60	2.18	1.70
d.o.f.	258	257	261	260

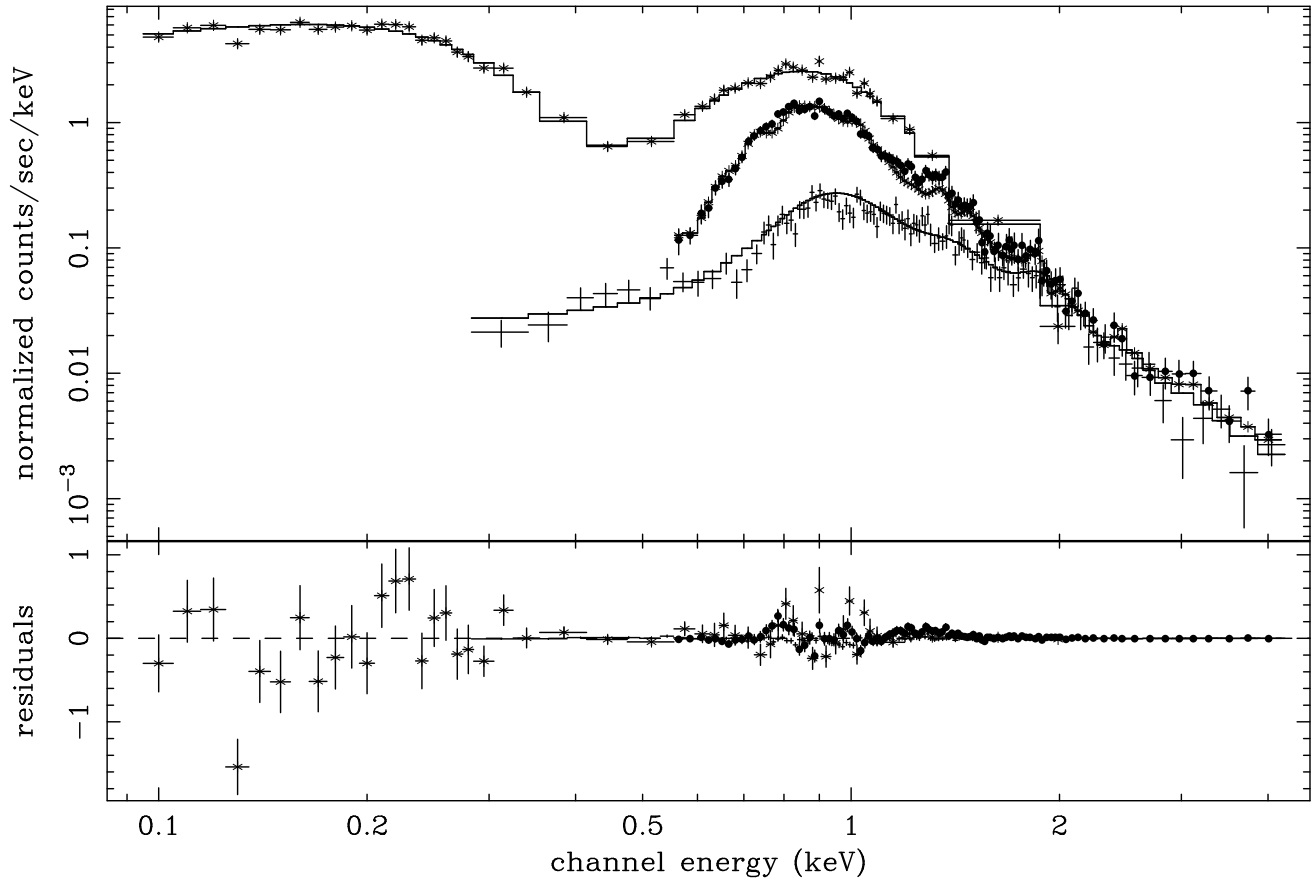

Fig. 3. Simultaneous fit of the two ASCA SIS0+GIS2 spectra and non-simultaneous ROSAT PSPC data with a 3T MK model with abundances free to vary in solar proportion. In this case the best–fit value is $Z = 0.35$.

(for a full discussion see Brickhouse et al. 1995). In any case, subsolar abundances on the order of $Z = 0.15 - 0.3$ are required to fit our ASCA–SIS data.

Not surprisingly, the analysis of the GIS data gives less clear results due to the lower spectral resolution and S/N. Statistically, the GIS data can equally be fitted by a 1T plasma with subsolar abundances or by a 2T plasma with abundances fixed at solar value. On the other hand, the ROSAT PSPC data seem to require a 2T model with subsolar abundances, although from these data alone it is not possible to properly constrain the temperatures, while the abundances are loosely determined to be between 0.2–0.6 the solar value. These results have been improved by simultaneous spectral fitting of data from different detector combinations. Analyzing together the best calibrated detectors, i.e. SIS0 and GIS2, simply confirms the results obtained with the SIS0 fits. We then widened the energy range by simultaneously fitting SIS0, GIS2 and ROSAT PSPC data (not simultaneous with the ASCA data). In this case, a third temperature is required to fit the data, confirming the results already found for other sources (e.g. Singh et al. 1995). We used 3T models with fixed solar abundances or abundances variable in solar proportion. Once again, we find that subsolar metal abundances, with values between 0.2 and 0.4, are required to fit the ROSAT+ASCA data. We can then conclude that all of our ASCA and ROSAT data show that the coronal plasma of HD 35850 is characterised by metal abundances lower than solar[1], on the order of $Z \approx 0.3$. This is in line with previous ASCA results. As a matter of fact, the ASCA data of active cool stars analysed so far point towards abundances typically in the range 0.1–0.3 of the solar value. These ASCA results are valid, in general, for very active and more evolved stars like the RS CVn and Algol binaries (White et al. 1994, White 1996; Singh et al. 1995, 1996; Ortolani et al. 1996). Nevertheless, low abundances have also been found in flare stars (Gotthelf et al. 1994, Mewe et al. 1996c) and, to a lesser extent, in single G/K–type stars (Drake et al. 1994). Furthermore, there is the case of AB Dor, a young star whose photospheric abundances are solar (Vilhu et al. 1987), but for which a metal poor corona, a factor 2–3 below solar, is required to fit simultaneous ASCA and EUVE spectra (White et al. 1996, Mewe et al. 1996b). And now we have the case of HD 35850, a young star whose photospheric

[1] We caution that the preliminary results presented by us elsewhere (which indicated a solar abundance for HD35850; Tagliaferri et al. 1996a,b) were based on a simplified analysis which included the channels below 0.55 keV. As discussed in Sect. 2.2, this has a crucial effect on the derived abundances.

abundances are also solar (Tagliaferri et al. 1994), but the corona is subsolar. So the general trend seems to be that more evolved, very active stars have low coronal metal abundances, while for the solar-type star EK Dra probably this is not the case (Güdel et al. 1996). These conclusions are not based on ASCA data alone, but also on GINGA (Tsuru et al. 1989; Stern et al. 1992) and, more recently, on ROSAT and EUVE data (e.g. Ottmann & Schmitt 1996; Kürster & Schmitt 1996; Singh et al. 1996; Stern et al. 1995; Rucinski et al. 1995; Mewe et al. 1996c; Schmitt et al. 1996).

The low spectral resolution of present X-ray detectors is not sufficient to resolve individual spectral lines, particularly in the Fe-L complex near 1 keV. This, combined with incomplete and possibly incorrect model line emissivities, can lead to erroneous abundance determinations (e.g. Liedahl et al. 1995) even if the effect is not so large to explain a reduction factor 3–5 in the abundances. However, all evidence points towards low metal abundances in very active stars. This seems to be a robust result, as it can not be fully ascribed to detector calibration problems. A tentative explanation can be given recalling the well known fact that coronal abundances in very active regions of the Sun are quite different from those in the photosphere. In particular, there is the so-called FIP (First Ionization Potential) effect. Elements having FIPs less than $\sim$ 10 eV are overabundant by typically a factor of four compared to those elements with higher FIPs (Meyer 1991; Feldman 1992). More recently, data obtained with the spacecraft Ulysses have shown that the FIP effect is much reduced in inactive regions (e.g. coronal holes) (Geiss et al. 1995). So already in the Sun there is a clear link between activity and metal abundances in the coronal plasma, but the situation is not at all clear and differences between different coronal structures or over time in the same regions have been detected (see Haisch et al. 1995 for a full discussion). However, in the case of active stars, no FIP effect has been seen so far (but see Güdel et al. 1996; Mg overabundant by a factor $\sim$ 2, while the other elements seem solar). Rather a general underabundance of most elements seems to prevail. This leads us to ask if there is a "saturation effect" also with respect to coronal elemental abundances.

To check if a FIP effect is present in the SIS data of HD 35850, we performed simultaneous SIS0+SIS1 spectral fits with 2T plasma models and abundances free to vary in non-solar proportions. We found quite a good agreement between the RS and MK models, with very low values of N, O and Ne. All other elements are around 0.2–0.3, except Ni, which has a high value in the RS model while it is more in line with the other elements in the MK model. So there could be an indication that elements with high FIP (N, O, Ne) are more depleted than the element with low FIP. However, the uncertainties both in the models and in the detector calibrations are such that we can not draw any conclusion at the present stage. In any case we note that, besides activity, age should also play a role, i.e. coronal elemental abundances are probably related both to the age and to the activity level of the star. For instance, the old but active Pop II binary HD 89499 presents a virtually metal free corona, i.e. still lower coronal abundances (Fleming & Tagliaferri 1996), in line with its very low photospheric metallicity due to its age. We may conclude by saying that the picture of metal abundance behaviour in the corona of active stars is still far from clear. To improve our understanding, we probably have to wait for the next generation of X-ray detectors with higher energy resolution and larger effective area, such as the gratings that will be on board the AXAF and XMM satellites.

As expected, two temperatures are necessary to fit the ASCA spectra and they seem very well constrained. If we consider the RS and MK results together for the various detectors, the softer component is between T = 0.4 – 0.7 keV, while the harder one is between T = 0.8 – 1.1 keV. These results are confirmed by the analysis of the ROSAT data, although with less constrained limits. These temperature values, in particular the hotter ones, are lower with respect to the values found for the RS CVn and Algol binaries (White et al. 1994; Antunes et al. 1994; Singh et al. 1995, 1996) and for AB Dor (White et al. 1996; Mewe et al. 1996b), but higher than other single G/K stars (Drake et al. 1994). Not only the plasma temperatures but also the total luminosity of this star is remarkable. The 0.5–2.0 keV luminosity is above $10^{30}\ erg\ s^{-1}$ in all of the three X-ray detections (EXOSAT, ROSAT and ASCA, spanning 9 years in time), an extremely high value for a single late F-type star (e.g. Fleming et al. 1989, 1995; Güdel et al. 1995; Schmitt 1996). This is an indirect confirmation that HD 35850 is a young, rapidly rotating object.

In the simultaneous fit of the ASCA+ROSAT data, a third temperature is required. However, this is not just an addition of a softer component, but is more a redistribution of the dominant temperatures, with a widening of the temperature range toward both lower and higher values. The harder component of the three is not very well constrained, with an uncertainty on the upper limit $\sim$ 100% on the best–fit value. In any case, the range spanned by the three temperatures seems not very large, from 5 to 15 million degrees, compared to the RS CVn and Algol binaries case. In our analysis, we also find that the RS model yields lower abundances and temperatures than the MK model. The differences are not very large, but are consistently present in the analysis of all detectors.

In conclusion, our data show that: i) HD 35850, a single F-type star, is a very active X-ray source; ii) its coronal plasma is characterised by low metal abundance values; iii) its X-ray emission is dominated by a coronal plasma with temperatures in the range of 5–15 million degrees.

Acknowledgements. GT and RP acknowledge partial support from the Italian Space Agency. FH thanks the Observatory of Merate for hospitality, and acknowledges financial support by the Swedish Natural Science Research Council. TAF acknowledges partial support from NASA grant NAG5-2955 under the ASCA guest observer program. We would like also to thank the referee Dr. R. Mewe for his useful comments.

References

Anders E., Grevesse N., 1989, Geochim. Cosmochim. Acta, 53, 197

Anders G.J., Innis J.L., Coates D.W., and Thompson K., 1991, MNRAS, 252, 408
Antunes A., Nagase F., White N.E., 1994, ApJ, 436, L83
Brickhouse, N.S., Raymond, J.C., Smith, B.W., 1995, ApJS, 97, 551
Cutispoto G., Tagliaferri G., Pallavicini R., Pasquini L., and Rodonó M., 1995, A&AS, 115, 1
Dempsey, R.C., Linsky, J.L., Schmitt, J.H.M.M., Fleming, T.A., 1993, ApJ, 413, 333
Drake, S.A., Singh, K.P., White, N.E., Simon, T., 1994, ApJ 436, L87
Favata, F., Barbera, M., Micela, G., Sciortino, S., 1993, A&A, 277, 428
Feldman, U., 1992, Phys. Scripta, 46, 202
Fleming, T.A., Gioia, I., and Maccacaro, T., 1989, ApJ, 340, 1011
Fleming, T.A., Liebert, J., Gioia, I., and Maccacaro, T., 1988, ApJ, 331, 958
Fleming, T.A., Schmitt, J.H.M.M., Giampapa, M.S., 1995, ApJ, 450, 401
Fleming, T.A., Tagliaferri, G., 1996, ApJ Lett, in press
Gagné, M., et al., 1996, in preparation
Gehrels N., 1987, ApJ, 303, 336
Geiss, J., Gloeckler, G., Von Steiger, R., 1995, Space Sience Rev., 72, 49
Gotthelf E.V., Jalota L., Mukai K., White N.E, 1994, ApJ, 436, L91
Güdel M., Guinem E.F., Mewe R., Kaastra J.S., Skinner S.L., 1996, ApJ, in press
Güdel M., Schmitt J.H.M.M., Benz A.O., 1995, A&A, 302, 775
Haisch, B., 1996, *IAU Colloquium No. 152: Astrophysics in the Extreme Ultraviolet* (eds S. Bowyer and R. Malina, Kluwer Academic Press)
Innis, J.L., Thompson, K., & Coates, D.W., 1986, MNRAS, 223, 183
Jeffries, R.D., 1995, MNRAS, 273, 559
Kürster, M., Schmitt, J.H.M.M., 1996, A&A, in press
Liedahl, D.A., Osterheld, A.L., Goldstein, W.H., 1995, ApJ, 438, L115
Mewe,R., Kaastra J.S., Liedahl D.A., 1996a, *Legacy* The Journal of the HEASARC, 6, 17
Mewe R., Kaastra J.S., van den Oord G.H.Y., Vink J., Tewara Y., 1996c, in press
Mewe R., Kaastra J.S., White, S.M., and Pallavicini, R., 1996b, A&A, in press
Meyer, J., 1991, Adv. Space Res., 11, 1, 269
Ortolani, A., Maggio, A., Pallavicini, R., Sciortino, S., Drake, J., Drake, S., 1996, in preparation
Ottmann, R., Schmitt, J.H.M.M., 1996, A&A, 307, 813
Pallavicini, R., Pasquini, L., and Randich, S., 1992a, A&A, 261, 245
Pallavicini, R., Randich, S., Giampapa, M.S., 1992b, A&A, 253, 185
Panarella A., Tagliaferri, G., Pallavicini, R. 1996, in 9^{th} *Cambridge Workshop on Cool Stars, Stellar Systems and the Sun* (eds R. Pallavicini and A.K. Dupree), in press
Pastori, L., Tagliaferri, G., 1996, in preparation
Randich, S., Gratton, G., Pallavicini, R., 1993, A&A, 273, 194
Raymond J.C., Smith B.W., 1977, ApJS, 35, 419
Rucinski, S.M., Mewe, R., Kaastra, J.S., Vilhu, O., White, S.M., 1995, ApJ 449, 900
Schmitt, J.H.M.M., 1996, A&A, in press
Schmitt, J.H.M.M., Stern, R.A., Drake, J.J., Kürster, M., 1996, ApJ 464, 898
Singh, K.P., Drake, S.A., White, N.E., 1995, ApJ 445, 840
Singh, K.P., White, N.E., Drake, S.A., 1996, ApJ 456, 766
Stern, R.A., Lemen, J., Schmitt, J.H.M.M., Pye, J.P. 1995, ApJ 444, l45
Stern, R.A., Uchida, R.A., Tsuneta, S., Nagase, F., 1992, ApJ 400, 321
Tagliaferri, G., Covino, S., Haardt, F., Fleming, T.A., Pallavicini, R., 1996a, in 9^{th} *Cambridge Workshop on Cool Stars, Stellar Systems and the Sun* (eds R. Pallavicini and A.K. Dupree), in press
Tagliaferri, G., Covino, S., Pallavicini, R., Uchida, Y., 1996b, in *X-Ray Imaging and Spectroscopy of Cosmic Hot Plasmas* (ed. F. Makino, Universal Academy Press, Japan) in press
Tagliaferri, G., Cutispoto, G, Giommi, P., Pallavicini, R., Pasquini, L., & Rodonò, M., 1992a, in 7^{th} *Cambridge Workshop on Cool Stars, Stellar Systems and the Sun* (eds M.S. Giampapa and J.A. Bookbinder), p. 122
Tagliaferri, G., Randich, S., Pallavicini, R., and Cutispoto, G., 1992b, in *High–resolution Spectroscopy with the VLT* (ed. M.–H. Ulrich), p. 171
Tagliaferri, G., Cutispoto, G., Pallavicini, R., Randich, S., & Pasquini, L., 1994, A&A, 285, 272
Tanakha, Y., Inoue, H., Holt, S.S., 1994, PASJ 46, L37
Tsuru, T., et al., 1989, PASJ, 41, 679
Vilhu, O., Gustafsson, B., & Edvarsson, B., 1987, ApJ, 320, 850
White, N.E., Arnaud, K., Day, C., et al., 1994, PASJ 46, L97
White N.E., 1996, in 9^{th} *Cambridge Workshop on Cool Stars, Stellar Systems and the Sun* (eds R. Pallavicini and A.K. Dupree), in press
White, S.M., Pallavicini, R., & Lim, J., 1996, in *Flares and Flashes* (eds J. Greiner, H.W. Duerbeck and R.E. Gershberg), p. 168

This article was processed by the author using Springer-Verlag LaTeX A&A style file *L-AA* version 3.